Theoretical Chemistry Accounts (2019) 138:122
https://doi.org/10.1007/s00214-019-2509-z

REGULAR ARTICLE

Theoretical study of the stability and NMR spectroscopic properties of vanadium(V) complexes

Lisset Noriega[1] · María Eugenia Castro[2] · Jose Manuel Perez-Aguilar[1] · Norma A. Caballero[3] · Thomas Scior[4] · Ramsés E. Ramírez[5] · Enrique González-Vergara[2] · Francisco Javier Meléndez[1]

Received: 22 February 2019 / Accepted: 30 September 2019 / Published online: 11 October 2019

Abstract

Several vanadium(V) complexes have been investigated as possible antidiabetic and anticancer therapeutic agents. Among these, vanadium(V) complexes linked to tridentate ONO Schiff bases stand out for their potential in the treatment for cancer. However, further studies are necessary in order to learn about their specific action at the cellular level. We investigate structural and spectroscopic properties of these particular complexes, which are formed by a Schiff base linked to a $[VO_2]^+$ ion that contains different functional groups. Molecular structure optimizations of these vanadium-containing complexes were performed by the ONIOM (QM1:QM2) method, where the high layer (complexes) were described by density functional theory methods whereas the low layer (eight water molecules) were described by the HF approach. Various solvation models were utilized; however, the introduction of both implicit (using a solvation model based on density, SMD) and explicit (eight water molecules) solvation improves the stability of the systems. Interestingly, we found that the location of the explicit water molecules in the different octahydrated vanadium complexes was conserved surrounding the oxo-vanadate moiety. A detailed analysis of the chemical shift (δ) values for ^{1}H, ^{13}C and ^{51}V is presented based on the ONIOM optimized geometries using the gauge-independent atomic orbital methodology. For obtaining accurately chemical shifts, the complete basis set using the correlation-consistent Dunning basis sets from double-ξ to quadruple-ξ and the Ahlrichs basis set were utilized. The results from the methodology presented here are consistent with those reported experimentally for ^{1}H. Again, the inclusion of explicit water molecules in the inner solvation shell during the calculation of the chemical shifts was crucial. The analysis of solvation energies also indicates the relevance of including explicit water molecules as the main stabilization factor suggesting the central role of intermolecular interaction in the stability of the metallic complexes. From this analysis, a possible vanadium complex candidate for further evaluation in the cellular environment is suggested. This work not only provides evidence of a suitable methodology for studying the structural and spectroscopic properties of vanadium complexes but also highlights the relevance of explicitly including water molecules in their inner shell.

Keywords Vanadium(V) complexes · Schiff bases · NMR spectroscopy · ONIOM method · CBS limit · Solvent effect

1 Introduction

Vanadium-containing complexes are of pharmacological interest, particularly those with V(IV) and V(V) oxidation states, due to their relatively low toxicity and high antidiabetic and anticancer activities [1–11], that are summarized in the scheme below. Schiff bases, a subclass of imine compounds with the R2C = NR general structure, are widely used in several research areas, including medicinal chemistry and biomedicine, because they can form complexes with different metals including vanadium, in their variety of oxidation states [12]. Despite their importance, the molecular mechanisms at atomic level need to be further investigated to advance in their development as possible pharmacological compounds (Scheme 1).

Published as part of the special collection of articles derived from the 11th Congress on Electronic Structure: Principles and Applications (ESPA-2018).

Electronic supplementary material The online version of this article (https://doi.org/10.1007/s00214-019-2509-z) contains supplementary material, which is available to authorized users.

✉ Francisco Javier Meléndez
francisco.melendez@correo.buap.mx

Extended author information available on the last page of the article

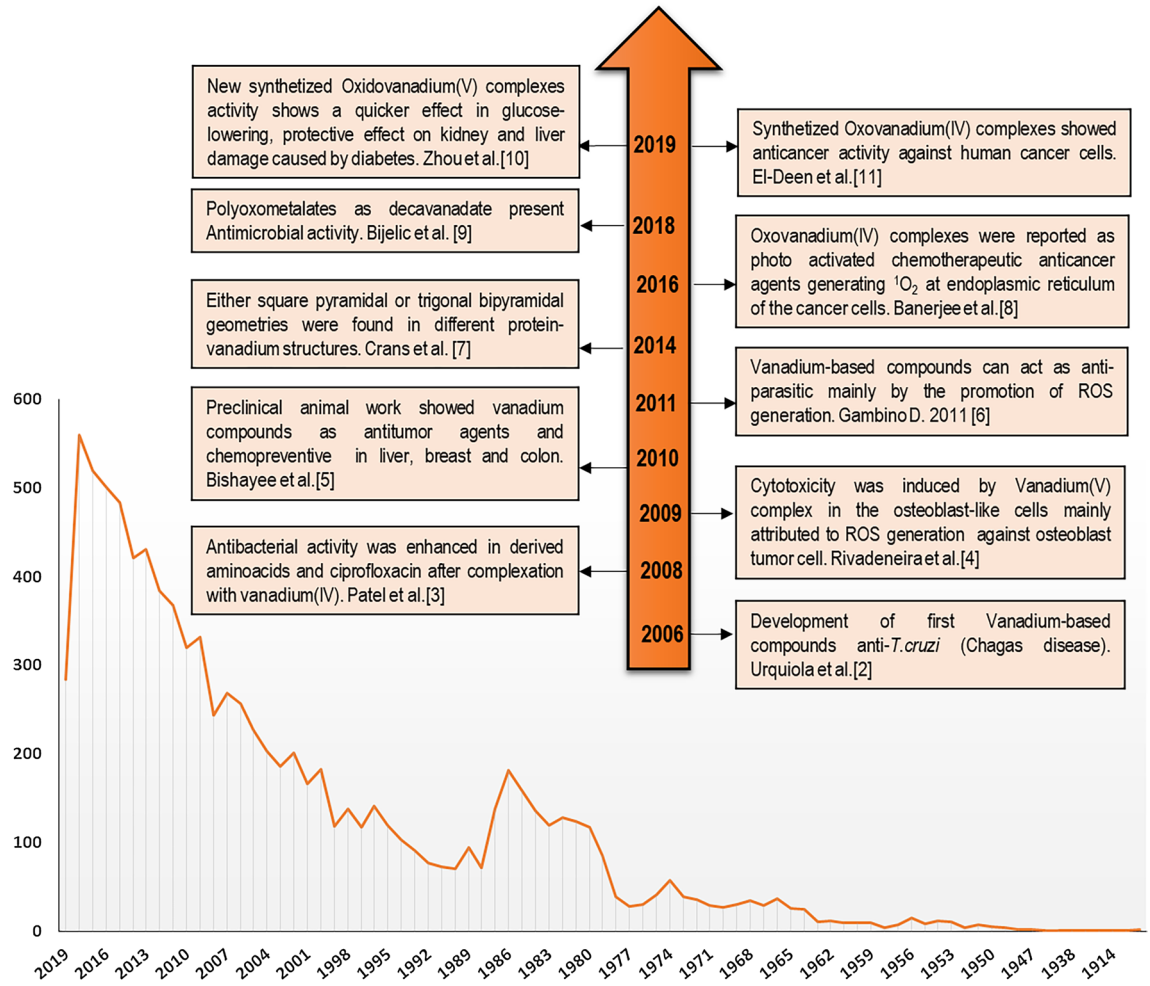

Scheme 1 A brief timeline of highlighted vanadium complexes applied in medicine field in recent years. Their applications mainly focus on their antidiabetic, antimicrobial and antitumoral properties. Below the timeline, a graphical representation of the number of publications through the years involving vanadium is presented. Data collected from PubMed

NMR is a versatile technique that provides information of the chemical environment of particular chemical bonds as well as the structure and dynamics of the molecular system. In addition, NMR also provides important information at an atomic level of interactions between metals and biomolecules [13]. Particularly in the study of vanadium-containing complexes and its behavior in biological systems, ^{51}V NMR is used to obtain information on the stability and changes associated with the nature of the ligands, providing insights for the investigation of systems formed by the vanadium atom linked to macromolecules [14].

Herein, a theoretical study of the NMR spectra of four vanadium(V) complexes, namely **VL1**–**VL4**, using the hybrid method ONIOM [15] with density functional theory (DFT) [16] and Hartree–Fock (HF) [17], is carried out in gas and solvation phases. One of the main aims is to learn how the chemical shift (δ) value of ^{51}V changes when the metal forms different complexes with the Schiff base (**L**) linked to the $[VO_2]^+$ ion [which forms part of the vanadium(V) complexes with anticancer activity], particularly in the presence of explicit water molecules and when the solvent effect is included implicitly in the system. The δ values were estimated using the complete basis set (CBS) limit [18] and the Dunning correlation-consistent [19] and Ahlrichs basis sets [20]. The CBS limit approach has been typically applied in the context of energy prediction [21–26] and previously by our group to predict electronic and free energies when metal complexes are surrounded by water molecules [27]. From our findings, we suggest a particular theoretical protocol consisting in introducing explicit water molecules in the inner solvation shell of the complex as well as using the CBS limit, to investigate the stability and spectroscopic NMR properties of metallic complexes.

Hence, we proposed the prediction of the ^{13}C and ^{51}V NMR chemical shifts for the octahydrated vanadium(V)

complexes containing the tridentate ONO Schiff base (**VL1**–**VL4**)·$(\mathbf{H_2O})_8$ using the CBS limit approach. In addition, the effect of implicit solvation by means of the solvation model based on density (SMD) [28] is analyzed.

2 Computational methodology

The optimized structure and vibrational frequencies, to ensure the global minimum of the ground state structures, were calculated with the ONIOM method [15], requesting two layers. In the first layer, we used the DFT theory with the M06-2X functional [29] and the cc-pVDZ basis set [19] for C, H, N, O, Cl atoms, and the LanL2DZ basis set for the V atom [30]. For V atoms, an effective core potential (ECP), namely a pseudopotential, was utilized to replace the core electrons. In the second layer, the calculations were carried out including the solvent effect by adding eight water molecules to the complexes (explicit solvation), that is, two water molecules per oxygen atom in the $[VO_2]^+$ ion and Schiff base, using the inner solvation shell model with HF approach [17]. Explicit solvation is based on previous studies on solvent effect when the first solvation shell is represented explicitly with small solvent molecules. Zhang et al. [31] used two-layer ONIOM QM/MM method for the evaluation of effect of six water molecules surrounding 2-aminopurine derivatives. Da Silva et al. [32] represented the first solvation shell in continuum solvation calculations using clusters of five solvent water molecules on 60 ionic species. The authors used as initial position, the structures obtained by molecular dynamics approaches and subsequently were completely relaxed using quantum mechanical calculations. In another work, the effect of water and ethanol on the structure of fluorophore molecule derivatives is tested with ONIOM QM/MM approach with four molecules of water and ethanol with the electronic embedding scheme [33]. In our case, the implicit solvent approach with the solvation model based on density (SMD) [28] was also used on octahydrated complexes (explicit + implicit solvation). NMR spectra calculations were performed from ONIOM (M06-2X/cc-PVDZ:HF/6-31G) [15] geometries using B3LYP functional [34] with the gauge-independent atomic orbital (GIAO) method [35]. Dunning correlation-consistent basis sets cc-pVDZ, cc-pVTZ, cc-pVQZ [19] and Ahlrichs TZVP [20] for C, H, O, N, Cl atoms, and LanL2DZ [30] for the V atom were used and extrapolated to the complete basis set (CBS) limit [18] for explicit + implicit solvation. The tetramethylsilane (TMS) molecule was used as a reference in the ^{1}H and ^{13}C NMR, and $VOCl_3$ for ^{51}V NMR spectra calculated using the same method and basis sets.

The extrapolated function for obtaining the CBS limit values for the δ (ppm) of (**VL1**–**VL4**)·$(\mathbf{H_2O})_8$ complexes, as well as the references used for calculating the NMR spectra, has the exponential form:

$$A(x) = A(\infty) + \mathrm{Be}^{-(x-1)} + \mathrm{Ce}^{-(x-1)^2} \quad (1)$$

where x is the cardinal number corresponding to basis set (2, 3, 4 for DZ, TZ and QZ) and $A(\infty)$ is the estimated CBS limit for δ when $x \rightarrow \infty$. In addition, for including a larger number of basis set, Ahlrichs TZVP was also included in the extrapolation.

Chemical shift (δ) values (ppm) were calculated using the following equation:

$$\delta\,(\mathrm{ppm}) = \sigma_{\mathrm{ref}} - \sigma_{\mathrm{i}} \quad (2)$$

where σ_{ref} is the isotropic magnetic shielding of the TMS and $VOCl_3$ references and σ_{i} is the isotropic magnetic shielding of the complexes with explicit solvation (**VL1**–**VL4**)·$(\mathbf{H_2O})_8$ and explicit + implicit solvation (**VL1**–**VL4**)·$(\mathbf{H_2O})_{8+\mathbf{SMD}}$· σ_{ref} and σ_{i} were obtained with the estimated CBS limit. All calculations were carried out using the Gaussian 09 program [36].

3 Results

3.1 Molecular structures

Four vanadium-containing complexes were investigated, **VL1**–**VL4**. In the case of the complex **VL1**, it is composed of the tridentate ONO Schiff base 1-(((5-chloro-2-oxidophenyl)imine)methyl)naphthalen-2-olate (**L**) and the $[VO_2]^+$ ion. As for the other complexes, **VL2**, **VL3** and **VL4** were studied by Ebrahimipour et al. [12]; one of the oxygen atoms from the dioxovanadium(V) ion (i.e., O_3 in Fig. 1) has different substituents attached, namely $-^+NH(CH_3CH_2)_3$, $-OCH_2CH_2CH_3$ and $-OCH_2CH_2CH_2CH_3$), respectively (see also Fig. 1). The crystallographic structures of the four compounds were obtained from the Cambridge Crystallographic Data Center (CCDC) database with reference numbers 1032428, 1032429, 1028790 and 1052671, respectively [37]. Additionally and for completeness, we also investigated the **VL1** system from the Schiff base **L** linked to $[VO_2]^+$ ion (see Fig. 1). Selected parameters for **L** and **VL1**–**VL4** calculated at M06-2X/cc-pVDZ in gas and DMSO phases are shown in Tables S1 and S2 in the Supplementary Materials (SM). Consistent results are obtained for **VL2**–**VL4** in both gas and DMSO phases with respect to the experimental data reported in [12], see Tables S1 and S2. Moreover, the M06-2X functional used in this study is known to be a reliable method for conformational studies, molecular structure and spectroscopy investigations [38]. Hence, the molecular structure of complex **VL1** was predicted with good confidence.

In order to evaluate the effect of the aqueous environment, the $[VO_2]^+$ ion in the complexes **VL1**–**VL4** was surrounded by eight water molecules in the inner solvation

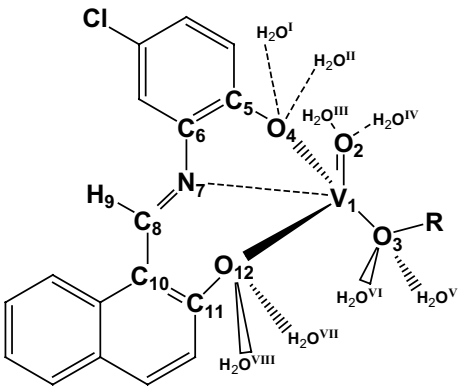

Complexes	R
VL1	---
VL2	$^{+}NH(CH_3CH_2)_3$
VL3	$CH_2CH_2CH_3$
VL4	$CH_2CH_2CH_2CH_3$

Fig. 1 Complex structures with the numbering convention for **L**, **VL1**–**VL4** and (**VL1**–**VL4**)·$(\mathbf{H_2O})_8$

shell, adding two water molecules per oxygen atom in the ion at a distance of 1.4 Å. The four octahydrated complexes: 1-(((5-chloro-2-oxidophenyl)imine)methyl)naphthalene-2-olate-di-oxido-vanadate(V)·$(H_2O)_8$ (**VL1**·$(\mathbf{H_2O})_8$), triethylammonium-1-(((5-chloro-2-oxidophenyl)imino)methyl)naphthalene-2-olate-di-oxido-vanadate(V)·$(H_2O)_8$ (**VL2**·$(\mathbf{H_2O})_8$), 1-(((5-chloro-2-oxidophenyl)imino)methyl)-naphthalen-2-olate-propoxido-oxido-vanadium(V)·$(H_2O)_8$ (**VL3**·$(\mathbf{H_2O})_8$) and 1-(((5-chloro-2-oxidophenyl)imino)methyl)-naphthalen-2-olate-butoxido-oxido-vanadium(V)·$(H_2O)_8$ (**VL4**·$(\mathbf{H_2O})_8$) were fully optimized. During the optimization, we used the two-layer ONIOM approach in both gas phase (**VL1**–**VL4**)·$(\mathbf{H_2O})_8$ and using the SMD implicit solvation model (**VL1**–**VL4**)·$(\mathbf{H_2O})_{8+SMD}$. The optimized structures for (**VL1**–**VL4**)·$(\mathbf{H_2O})_{8+SMD}$ are depicted in Fig. 2.

With the aim of exploring the electronic energies tendencies for complexes in different water solvation models, the electronic energies were compared between (**VL1**–**VL4**) in gas phase, implicit model solvation by the SMD model (**VL1**–**VL4**)$_{SMD}$, explicit solvation (**VL1**–**VL4**)·$(\mathbf{H_2O})_8$, and implicit + explicit model (**VL1**–**VL4**)·$(\mathbf{H_2O})_{8+SMD}$. These energies are shown in Fig. 3, in which the lowest energy corresponds to the (**VL1**–**VL4**)·$(\mathbf{H_2O})_{8+SMD}$ complexes, showing energy differences compared with (**VL1**–**VL4**)·$(\mathbf{H_2O})_8$ of 72, 53, 45 and 35 kcal mol^{-1} for **VL1**, **VL2**, **VL3** and **VL4**, respectively. These results indicate that by considering explicit + implicit solvation, all the systems improve their energy stability. However, the most significant improvement comes from the explicit addition of the water molecules (see Fig. 3).

The selected parameters for the complexes (**VL1**–**VL4**)·$(\mathbf{H_2O})_{8+SMD}$ are shown in Table 1. The

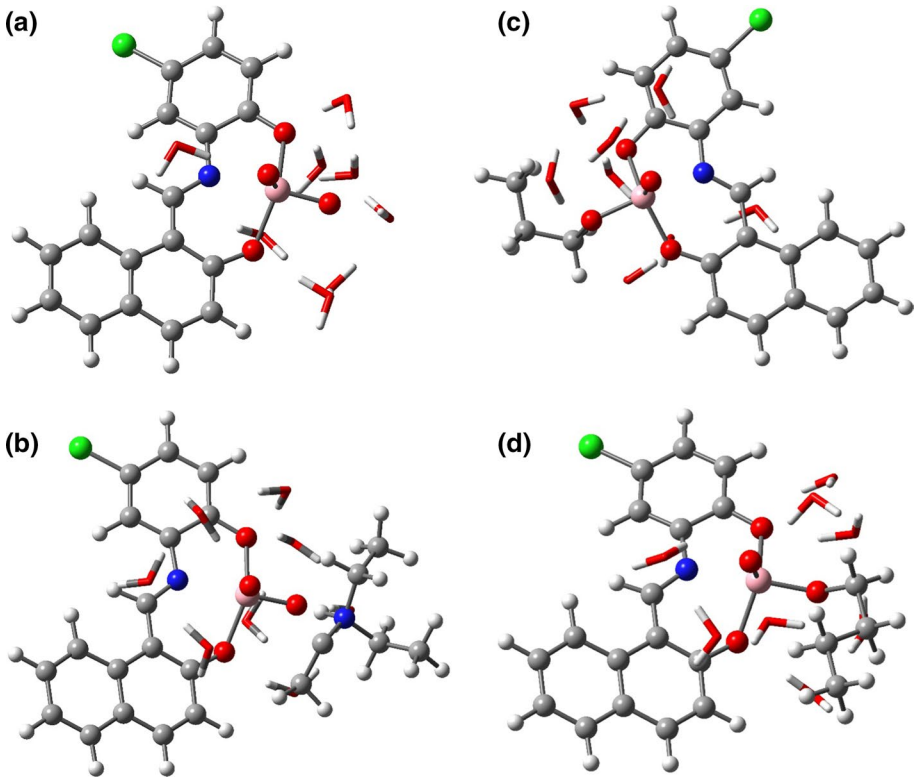

Fig. 2 Octahydrated vanadium(V) complexes linked to the Schiff base with SMD: (a) **VL1**·$(\mathbf{H_2O})_{8+SMD}$, (b) **VL2**·$(\mathbf{H_2O})_{8+SMD}$, (c) **VL3**·$(\mathbf{H_2O})_{8+SMD}$, (d) **VL4**·$(\mathbf{H_2O})_{8+SMD}$. Color code is as follows: C atoms in gray, H atoms in white, O atoms in red, N atoms in blue, Cl atoms in green and V atoms in pink

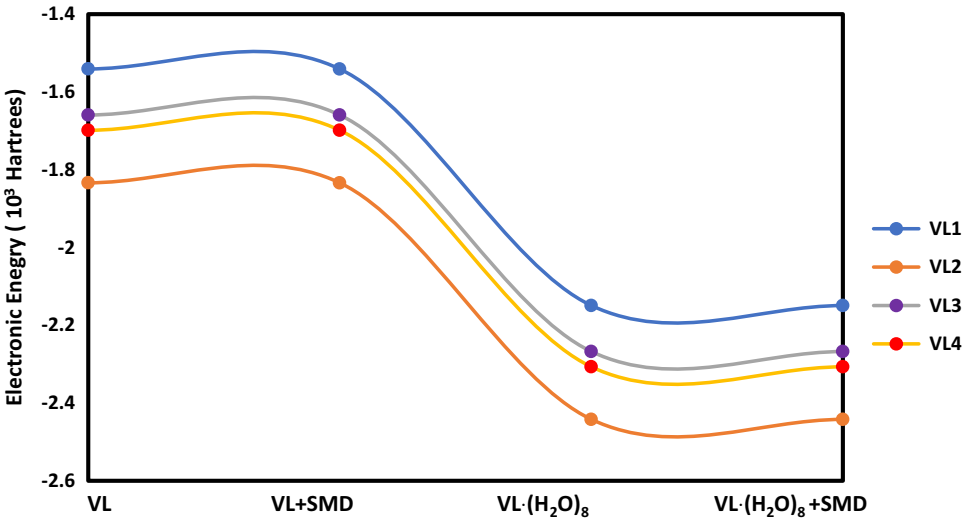

Fig. 3 Energies for the **VL1**–**VL4** complexes (in 10^{-3} Hartrees) in gas and different solvation models

numbering convention is in agreement with Fig. 1. Atom N_{13} refers to the N atom in $-^{+}NH(CH_3CH_2)_3$ substituent in **VL2**, and atom C_{13} refers to first C atom in the substituents $–CH_2CH_2CH_3$ and $–CH_2CH_2CH_2CH_3$ in **VL3** and **VL4**, respectively. By comparing these parameters with those from the octahydrated complexes (**VL1**–**VL4**)·$(\mathbf{H_2O})_8$ (see Table S3 in SM), we observed similar values for bond distances and angles; however, two bond angles, O12–V1–O4 and O3–V1–N7, are significantly changed in the octahydrated compounds. These angles are important during the calculation of the τ parameter, which is an index of degree of distortion of square pyramid metal arrangement ($\tau = 0$); as τ approaches to 1, the metal conformation approaches a trigonal bipyramid structure. In the (**VL3**, **VL4**)·$(\mathbf{H_2O})_{8+SMD}$ complexes, the square pyramid is more distorted compared to the (**VL3**, **VL4**)·$(\mathbf{H_2O})_8$ counterparts, whereas the (**VL1**, **VL2**)·$(\mathbf{H_2O})_{8+SMD}$ structures are less distorted when the SMD is applied to the octahydrated complexes. This last finding may be directly related with difference in the electrostatic nature of the complexes. These distortions also have influence in other angles like O2–V1–O4 and O2–V1–O4 that are part of the square pyramid.

O–H_2O distances placed at 1.4 Å as initial guess are obtained in a range of 1.95–3.91 Å after full optimization was performed considering the SMD. The average value for the distance of the vanadium atom to the water molecules [closest hydrogen atom; $(V1–H_2O)_{average}$] is found to have similar values between 4.05 and 4.25 Å for the four octahydrated complexes calculated with SMD; these distance values are similar to the those obtained in the absence of the implicit solvation.

On the other hand, due to conformational flexibility of the alkyl groups in the **VL3** and **VL4** complexes, $–CH_2CH_2CH_3$ and $–CH_2CH_2CH_2CH_3$, respectively, a conformational search was carried out along the V1–O3–C13–C14 dihedral angle in both **VL3**·$(\mathbf{H_2O})_{8+SMD}$ and **VL4**·$(\mathbf{H_2O})_{8+SMD}$. The **VL3**·$(\mathbf{H_2O})_{8+SMD}$ complex had two minima in potential energy curve: the global minimum, which is considered in this study, and a local minimum with an energy difference of -4.22 kcal mol^{-1}. The main structural differences among these **VL3**·$(\mathbf{H_2O})_{8+SMD}$ minima are located in the torsional angles formed by V1–O3–C13–H16 and O3–C13–C14–C15 (propoxy radical). The τ value also changed slightly in both global and local minima, 0.36 and 0.23, respectively. In the case of the **VL4**·$(\mathbf{H_2O})_{8+SMD}$ complex, we did not find additional local minima on the potential energy curve.

Complexes were fitted using VMD molecular graphics viewer [39] in order to know the location of the optimized water molecules in the different complexes. The color code for the complexes is the same as in Fig. 4: **VL1**—blue, **VL2**—orange, **VL3**—purple and **VL4**—red. The moiety corresponding to the Schiff base was hidden for clarity. It can be observed that: (1) water molecules are mainly surrounding the oxo-vanadate, particularly the O_2 atom, see Fig. 1 for numbering convention; (2) water molecules are located in a similar positions in the **VL1**, **VL2** and **VL4** complexes. In the case of the **VL3** complex (purple), the location of the water molecules is somehow different relative to the other complexes, yet the water molecules still surround the oxo-vanadate moiety, and (3) the slightly different position between the water of the different complexes is attributed, as expected, to steric effects of the of different substituents.

3.2 NMR calculations

The chemical shifts (δ) for the ^1H NMR spectrum using the CBS-B3LYP method with different basis sets for the **VL1**–**VL4** complexes in DMSO phase are shown in the

Table 1 Selected optimized parameters for the complexes (**VL1**–**VL4**)·$(\mathbf{H_2O})_{\mathbf{8+SMD}}$ at the ONIOM (M06-2X/cc-PVDZ:HF/6-31G) theory level with SMD solvation. Bond lengths in (Å) and angles in (°)

Parameter	VL1·$(H_2O)_{8+SMD}$	VL2·$(H_2O)_{8+SMD}$	VL3·$(H_2O)_{8+SMD}$	VL4·$(H_2O)_{8+SMD}$
O4–C5	1.34	1.34	1.34	1.34
O12–C11	1.32	1.32	1.33	1.33
N7–C8	1.30	1.30	1.30	1.30
N7–C6	1.41	1.41	1.41	1.41
Cl–C	1.75	1.75	1.75	1.75
V1–O4	1.94	1.94	1.89	1.89
V1–O12	1.92	1.92	1.87	1.86
V1–O3	1.61	1.63	1.76	1.75
V–O2	1.62	1.60	1.56	1.56
V1–N7	2.21	2.20	2.13	2.18
C10–C8–N7	124.3	124.4	124.39	123.51
C8–N7–C6	121.7	121.4	121.98	122.76
C10–C11–O12	123.9	123.1	122.22	122.36
C6–C5–O4	117.9	118.0	116.77	117.01
N7–C6–C5	111.8	111.9	111.40	111.33
C8–C10–C11	120.5	119.8	119.55	119.76
O2–V1–O3	108.8	108.1	107.55	105.76
O2–V1–O12	106.6	105.1	110.65	109.83
O2–V1–O4	106.6	105.8	108.25	108.96
O2–V1–N7	95.3	99.6	93.92	90.60
O3–V1–O4	92.9	94.0	92.39	92.47
O3–V1–O12	96.0	94.8	93.61	99.27
O12–V1–N7	80.5	79.6	81.40	80.11
O4–V1–N7	75.9	76.3	77.52	76.36
O12–V1–O4	140.6	143.4	136.6	134.36
O3–V1–N7	155.6	152.3	158.3	162.63
V1–O4–C5–C6	−15.9	−7.5	16.8	−14.08
V1–O12–C11–C10	29.3	36.4	−36.9	39.20
N7–C6–C5–C4	−178.6	−178.6	179.0	−179.19
N7–C8–C10–C11	−9.6	−12.2	13.9	−15.09
C6–N7–V1–O3	−77.4	−76.8	78.5	−62.80
N7–V1–O3–N13	–	−175.0	–	–
O3–N13–C14–C15	–	174.3	–	–
O2–V1–O3–N13	–	9.1	–	–
N7–V1–O3–C13	–	–	17.0	162.88
O3–C13–C14–C15	–	–	66.2	−66.02
O2–V1–O3–C13	–	–	−171.7	3.14
O4–H_2O I	2.0	2.09	3.9	2.10
O4–H_2O II	2.11	2.00	2.22	2.02
O2–H_2O III	1.98	2.01	3.20	2.23
O2–H_2O IV	2.01	3.56	2.22	2.31
O3–H_2O V	1.97	1.95	2.09	3.34
O3–H_2O VI	3.38	3.34	2.45	2.96
O12–H_2O VII	2.12	1.98	2.23	2.28
O12–H_2O VIII	2.14	3.81	2.32	3.92
(V1–H_2O)$_{average}$	4.05	4.25	4.25	4.20
(O–H_2O)$_{average}$	3.09	3.37	3.34	3.40

Table S4. Calculated values display good correlation with experimental values reported previously [12], with correlation coefficients values of $R^2 = 0.9409$, 0.9813 and 0.9919, for the complexes **VL2**–**VL4** in DMSO solution, respectively. The correlation parameters between the experimental and theoretical results are collected in Table S5, showing a good correlation for the ^{1}H NMR data in DMSO solution. Hence, we propose that the methodology using GIAO with (M06-2X/cc-PVDZ:HF/6-31G)//CBS-B3LYP is reliable enough to be used in further analysis. Using this methodology, values of δ_{teo} of ^{1}H NMR for the **VL1** complex were accurately predicted.

In Table S6, it can be observed that estimated CBS limits of δ_{calc} for the (**VL1**–**VL4**)·$(\mathbf{H_2O})_8$ systems using the TMS reference, $\sigma_{TMS} = 31.26$ ppm, are in general shifted to upfield regions when compared with the values of the **VL1**–**VL4** complexes in DMSO (Table S4). This effect is more evident in the case of the $\mathbf{H_{CH=N}}$ proton, since NMR results are susceptible to structural changes. Thus, we expected a significant change in δ in this particular hydrogen atom when water molecules are explicitly taken into account, because it is bounded to a carbon atom that is bound to a nitrogen atom that is part of the distorted square pyramid. However, the chemical shift from the ^{1}H NMR data in the (**VL1**–**VL4**)·$(\mathbf{H_2O})_{\mathbf{8+SMD}}$ complexes moves slightly downfield, although it seems to have a chemical behavior similar to the ones obtained experimentally, see Table S7. Thus, we suggest that considering explicit + implicit water solvation results in a better approximation to the chemical behavior of the metallic complexes.

The predictions of the δ for the ^{13}C and ^{51}V NMR data are shown in Tables S8, S9 and Tables 2, 3. For the octahydrated

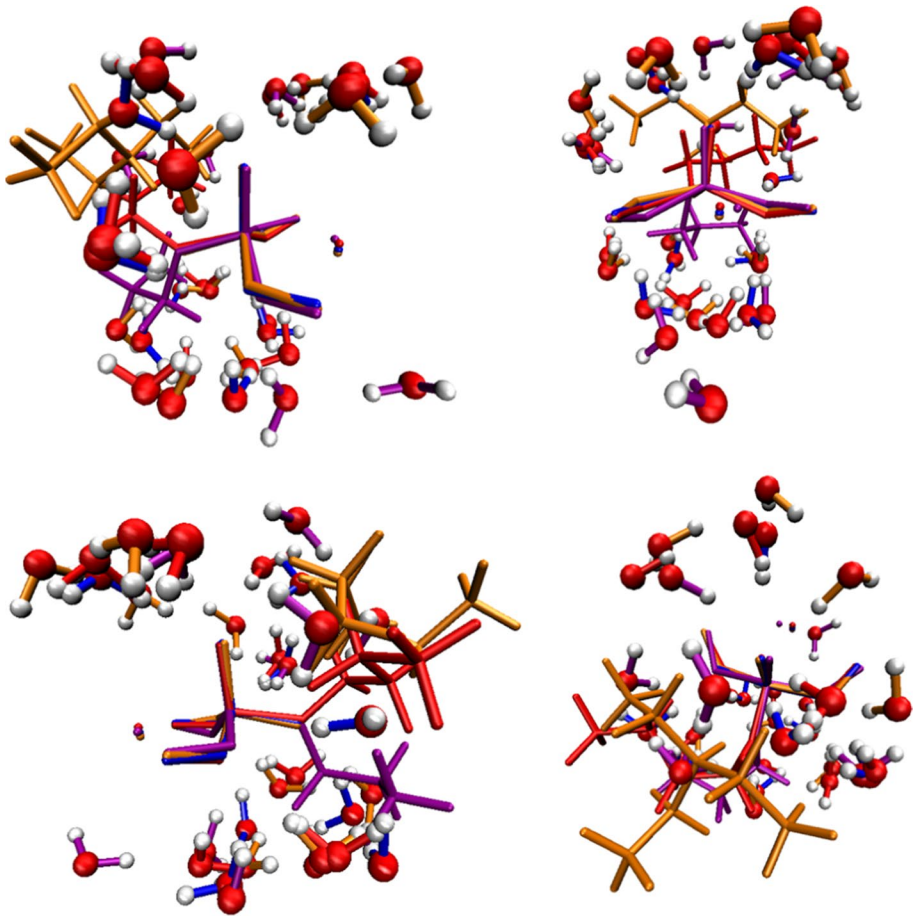

Fig. 4 Different views of **VL**s fitted illustrating the positions of water molecules surrounding the complexes. **VL1** in blue, **VL2** in orange, **VL3** in purple and **VL4** in red

Table 2 ^{13}C NMR chemical shifts (δ) in ppm for the complexes (**VL1**–**VL4**)·($\mathbf{H_2O}$)$_{\mathbf{8+SMD}}$ using the CBS-B3LYP method including aqueous solvation with SMD

VL·(H_2O)$_8$	Assignment	δ TZVP	δ cc-pVDZ	δ cc-pVTZ	δ cc-pVQZ	δ_H CBS est.	σ_{TMS} CBS est.
VL1·($\mathbf{H_2O}$)$_{\mathbf{8+SMD}}$	C_{ring}	120.3–177.4	115.2–167.2	118.8–176.5	122.0–179.7	117.6–170.7	190.851
	$C_{CH=N}$	157.0	149.4	157.3	160.6	153.0	
VL2·($\mathbf{H_2O}$)$_{\mathbf{8+SMD}}$	C_{ring}	120.1–170.5	115.3–160.2	120.1–170.0	122.5–172.8	117.8–163.5	190.851
	$C_{CH=N}$	158.1	149.4	157.2	161.1	153.2	
	$C_{+NH(CH3CH2)3}$	5.7–53.0	7.0–52.7	5.9–53.7	6.3–54.9	7.2–54.0	
VL3·($\mathbf{H_2O}$)$_{\mathbf{8+SMD}}$	C_{ring}	119.1–177.0	115.4–167.3	120.0–176.7	122.6–179.6	118.3–170.7	190.851
	$C_{CH=N}$	159.5	151.0	159.0	162.5	154.6	
	$C_{(CH2)2CH3}$	15.8–88.3	16.7–85.3	16.1–87.6	16.5–88.8	17.1–86.3	
VL4·($\mathbf{H_2O}$)$_{\mathbf{8+SMD}}$	C_{ring}	120.2–177.3	115.8–167.8	121.0–176.9	123.4–179.8	118.6–171.1	190.851
	$C_{CH=N}$	157.7	149.1	157.1	160.5	152.6	
	$C_{(CH2)3CH3}$	16.3–101.5	17.8–96.9	17.1–100.7	17.6–102.0	18.3–98.1	

complexes, (**VL1**–**VL4**)·($\mathbf{H_2O}$)$_{\mathbf{8}}$, all the δ values for the carbon atoms from the CBS estimation of the aromatic ring, C_{ring}, are found at the 115.4–171.7 ppm range, whereas for the carbon at the imine group, $C_{CH=N}$, the values are in the 143.1–151.1 ppm range. For carbon atoms in the R substituents, the δ values in the case of the aliphatic –$(CH_2)_2CH_3$ and –$(CH_2)_3CH_3$ substituents are 14.7 and 98.8 ppm for **VL3**·($\mathbf{H_2O}$)$_{\mathbf{8}}$ and **VL4**·($\mathbf{H_2O}$)$_{\mathbf{8}}$, while for –$^{+}$NH$(CH_3CH_2)_3$ substituent, the δ_{calc} values are predicted at the range of 6.0–54.8 ppm for the **VL2**·($\mathbf{H_2O}$)$_{\mathbf{8}}$ complex, see Table S8. In aqueous solution, shift to downfield was found in δ_{calc} values around 5 and 10 ppm, for the C_{ring} and $C_{CH=N}$ atoms, respectively. For carbon atoms, the R substituents are also slightly shifted downfield for (**VL3**–**VL4**)·($\mathbf{H_2O}$)$_{\mathbf{8+SMD}}$

Table 3 ^{51}V NMR chemical shifts (δ) in ppm for the complexes (**VL1**–**VL4**)·(**H$_2$O**)$_{8+SMD}$ using the CBS-B3LYP method and the aqueous solvation model with SMD

VL·(H$_2$O)$_8$	δ TZVP	δ cc-pVDZ	δ cc-pVTZ	δ cc-pVQZ	δ CBS est.	σ_{VOCl3} CBS est.
VL1·(H$_2$O)$_{8+SMD}$	−577.2	−544.2	−534.9	−506.8	−508.0	−2952.64
VL2·(**H$_2$O**)$_{8+SMD}$	−593.4	−551.8	−548.3	−520.4	−515.6	
VL3·(**H$_2$O**)$_{8+SMD}$	−521.0	−472.9	−479.4	−456.3	−442.9	
VL4·(**H$_2$O**)$_{8+SMD}$	−527.1	−476.7	−485.1	−463.9	−448.3	

complex with chemical shift values no larger than 3.0 ppm. The changes observed for the complex **VL2**·(**H$_2$O**)$_8$ could be attributed to the charge–charge interactions found for $^{+}$NH(CH$_3$CH$_2$)$_3$ and $^{-}$OVOL·(H$_2$O)$_8$ moieties, see Table 2.

On the other hand, Tables S9, S10 and 3 contain the results for the ^{51}V NMR spectra. From the CBS estimation, the δ ^{51}V values are predicted to range between −458.3 and −532.2 ppm in the case of the (**VL1**–**VL4**)$_{SMD}$ complexes with the aqueous SMD solvation, see Table S9. When the solvation effect is taken into account via the SMD approach and water molecules are also included explicitly, the δ ^{51}V values change to a range between −442.9 and −515.6 ppm in the case of the (**VL1**–**VL4**)·(**H$_2$O**)$_{8+SMD}$ complexes, see Table 3. In the absence of the implicit aqueous model, that is, for the (**VL1**–**VL4**)·(**H$_2$O**)$_8$ complexes (in Table S10), the differences in the chemical shift are smaller than 20 ppm relative to the (**VL1**–**VL4**)·(**H$_2$O**)$_{8+SMD}$ complexes. This shift to the upfield region is caused only by the inclusion of the implicit effect of the solvent. It is noteworthy that the δ_{calc} for the ^{13}C atoms does not display any tendency for any of the complexes and for any of the basis set. Yet, by using the CBS limit for extrapolating the δ NMR values ensures that the calculated chemical shifts are correctly predicted. In general, the results for the δ ^{51}V NMR when only the implicit solvent model is included exhibit a trend toward downfield values for the (**VL1**–**VL4**)$_{SMD}$ complexes with an increase in the size of basis set, see Table S9. However, for the octahydrated complexes, (**VL1**–**VL4**)·(**H$_2$O**)$_8$, the calculations show a trend toward downfield regions when the cc-pVDZ and cc-pVTZ basis sets are used. Finally, from Table 3, using explicit + implicit model, the complexes (**VL3**, **VL4**)·(**H$_2$O**)$_{8+SMD}$ also present similar variations but to a larger extent. Since when using the CBS extrapolated function, the differences and contributions for all the basis sets are considered, we observed that all the values of δ ^{51}V are balanced out.

In this form, the CBS approach allows us to estimate the δ ^{51}V with reliability for the three solvation approximations. According to our results, when different solvation models are tested, see Tables S9, S10 and 3, we suggest that using the CBS approach together with implicit + explicit solvation models produces the best results, and thus, it is an adequate methodology for dealing with these vanadium(V) complexes.

Spectroscopic data of δ ^{51}V NMR in DMSO-d$_6$ of oxovanadium(V) complexes have been reported in a range of −469 to −550 ppm [40–45] (see Table 4). On the other hand, Melendez and coworkers carried out a theoretical NMR study dealing with vanadate complexes. In that study, they obtained reliable results for δ values of ^{1}H, ^{13}C and ^{51}V in gas phase; D$_2$O; and DMSO-d$_6$ solvents using the B3LYP functional [40]. In this case and in aqueous solution, the δ ^{51}V were found at a range of −784 to −786 ppm, while the experimental data was reported at −748 to −754 ppm where the only water molecule explicitly placed in the systems interacts with a bis-peroxo-oxovanadate ion [46]. It would be interesting to analyze the effect of surrounding the [VO(O$_2$)$_2$·(H$_2$O)]$^{-}$ chemical moiety with water molecules to assess the capacity of the explicit solvent to move the ^{51}V chemical shift values to upfield regions.

3.3 Solvation energies

The ongoing development of implicit solvent models for the accurate prediction of the solvation free energies (ΔG^{solv} denoting transfer of solute at 298.15 K from 1.0 mol L^{-1} in the ideal gas phase to 1 mol L^{-1} in the ideal dilute solution phase) is focused on their importance in better understanding and estimating processes related to equilibria in solution, biological partitioning, and so on which are fundamental aspects of molecular biology and medicinal chemistry [47, 48]. The theoretical solvation energy estimation is frequently used to support the experimental measurements due to the difficulties related with the nature of the experimental characterization. In this work, the solvation free energies of the Schiff base **L**, the complexes **VL1**–**VL4** and the octahydrated complexes (**VL1**–**VL4**)·(**H$_2$O**)$_8$ were calculated from the gas to the solution phase using the SMD model. The results are shown in Tables 5 and 6.

In the Table 5, it is observed that **VL1**, **VL2** and **VL4** are more stable in aqueous phase, while in the case of **VL3**, our results indicate that it presents similar stability in both solution phases. In the aqueous phase, the VL complexes present the following trend in stability: **VL3** < **VL4** < **VL2** < **VL1**. By explicitly including water molecules in the inner solvation shell to generate the octahydrated complexes (**VL1**–**VL4**)·(**H$_2$O**)$_8$, a significant stabilization is observed in the

Table 4 Spectroscopic data of ^{51}V NMR in DMSO-d6 of oxovanadium(V) complexes linked to the Schiff bases

Complex	δ (ppm)	Refs.
(*S*-Benzyl-3-((3-oxy-5-hydroxymethyl-2-methylpyridinium-4-yl)methylidene)dithiocarbazato)-dioxovanadium(V)	−469.6	[41]
$C_{16}H_{16}N_3O_4S_2V$		
2-(2,5-Diaza-1-hexen-1-yl-κ^{2}N)-4-nitrophenolatoκO-dioxovanadium(V)	−528.7	[42]
$C_{10}H_{12}N_3O_5V$		
(2-(((2-Oxy-3,5-bis(t-butyl)benzylidene)amino)methyl)-4,5,6-trimethoxytetrahydro-2*H*-pyran-3-olato)-(methanolato)-oxovanadium(V)	−535.0	[43]
$C_{25}H_{40}NO_8V$		
(N-Salicylidene-2(benzimidazole-2-yl) ethylamine)-cis-dioxovanadium(V)	−540.3	[44]
$C_{16}H_{14}N_3O_3V$		
{R(-)-2-amino-1-*N*-[(2′-oxido-κO-4′,6′-dimethoxyphenyl) methylene] aminopropane-κ^{2}N}dioxidovanadium(V)	−550.3	[45]
$C_{12}H_{17}N_2O_5V$		
Glycine-L-histidine-bis-peroxovanadato	−782.9	[40]
[$VO(O_2)_2\cdot(H_2O)$] GH		
Glycine-glycine-L-histidine-bis-peroxovanadato	−783.8	[40]
[$VO(O_2)_2\cdot(H_2O)$] GGH		
Glycine-L-histidine-glycine-bis-peroxovanadato	−785.0	[40]
[$VO(O_2)_2\cdot(H_2O)$] GHG		

Color code: carbon—gray, nitrogen—blue, oxygen—red, sulfur—yellow, vanadium—pink

Table 5 Solvation free energies (in kcal mol^{-1}) for the complexes **VL1**–**VL4** with the ONIOM (M06-2X/cc-PVDZ:HF/6-31G) theory level

VL	$\Delta G^{\text{Solv-H}_2\text{O}}$	$\Delta G^{\text{Solv-DMSO}}$
VL1	−63.0	−54.93
VL2	−26.91	−24.75
VL3	−17.16	−16.84
VL4	−17.08	−16.55

$\Delta G^{\text{Solv}} = (G_{\text{SMD}} - G_{\text{Gas phase}})$

Table 6 Solvation free energies (in kcal mol^{-1}) for octahydrated complexes (**VL1**–**VL4**)·$(H_2O)_8$ with the ONIOM M06-2X/cc-PVDZ:HF/6-31G theory level

VL·$(H_2O)_8$	$\Delta G^{\text{Solv-H}_2\text{O}}$
VL1·$(H_2O)_8$	−79.27
VL2·$(H_2O)_8$	−62.62
VL3·$(H_2O)_8$	−55.55
VL4·$(H_2O)_8$	−48.31

$\Delta G^{\text{Solv}} = (G_{\text{SMD}} - G_{\text{Gas phase}})$

Table 6 by about −48.31 to −79.27 kcal mol^{-1}, with the following trend: **VL4**·$(H_2O)_8$ < **VL3**·$(H_2O)_8$ < **VL2**·$(H_2O)_8$ < **VL1**·$(H_2O)_8$. This suggests that the intermolecular interactions, namely hydrogen bonds, provide significant stabilization to the complexes. In general, it could be suggested that the octahydrated complexes are more stable when they are additionally embedded in implicit water solvation models, as was observed in previous studies of vanadium-containing complexes in aqueous solution [49]. In particular, the complex **VL2**·$(H_2O)_8$ presents the most stable ΔG^{Solv} with respect to the reference complex **VL1**·$(H_2O)_8$ (without substituent), which could be attributed to the presence of a net charge in the moieties. Therefore, it could be a possible candidate to be evaluated in biological systems (aqueous phase).

4 Conclusions

Therapeutically relevant vanadium-containing complexes were investigated using theoretical approaches. The particular role of different levels of solvation models (i.e., implicit, explicit or a combination of both), particularly around the $[VO_2]^+$ ion, was evaluated. We found that by including implicit + explicit solvation, the stability of all the systems improves. Yet such improvement was mainly driven by the addition of explicit water molecules. Interestingly, in the case of the octahydrated compounds, significant distortions of square pyramid metal arrangement were observed. Moreover, the location of the water molecules around the metallic complexes adopted similar positions surrounding the oxo-vanadate moiety. We suggest that the optimization protocol followed in this study is appropriate for investigating metallic complexes.

The chemical shift (δ) values for ^{1}H, ^{13}C and ^{51}V were calculated using the complete basis set (CBS) limit approach. From our analysis of the different solvation models, we suggest that considering explicit + implicit water solvation results in a better approximation to the chemical behavior of the metallic complexes. Furthermore, we concluded that values obtained using the methodology for ^{1}H (explicit water molecules in the inner solvation shell and the

CBS limit for extrapolating the δ NMR values) are consistent with experimental results, which provides further confidence in the results obtained for ^{13}C and ^{51}V cases.

Lastly, the analysis of the solvation energies indicates that the inclusion of the explicit water in the inner shell is the main stabilization factor. This suggests that the intermolecular interactions, specifically hydrogen bonds, provide significant stabilization to the metallic complexes.

Finally, our results suggest a particular theoretical protocol involving the introduction of explicit water molecules in the inner solvation shell and the CBS limit, as a suitable methodology for studying metallic complexes and the NMR spectroscopic properties.

5 Supplementary material

Table S1: Selected optimized parameters for the Schiff base **L-*trans*** and the complexes **VL1–VL4** with the M06-2X/cc-pVDZ theory level in the gas phase; Table S2: Selected optimized parameters for the Schiff base **L-*trans*** and the complexes **VL1–VL4** with the M06-2X/cc-pVDZ theory level in the DMSO phase; Table S3: Selected optimized parameters for the complexes (**VL1–VL4**)·(**H_2O**)$_8$ ONIOM (M06-2X/cc-PVDZ:/HF/6-31G) theory level in gas phase; Table S4: ^1H NMR isotropic magnetic shielding (σ) and chemical shifts (δ) in ppm, for the Schiff base L and the complexes **VL1–VL4** with the CBS-B3LYP method in DMSO solution; Table S5: Correlation parameters between experimental and theoretical ^1H NMR chemical shifts (ppm) for **L-*trans*** and the complexes **VL2–VL4** in gas and DMSO phase; Table S6: ^1H NMR isotropic magnetic shielding (σ) and chemical shifts (δ) in ppm for the complexes (**VL1–VL4**)·(**H_2O**)$_8$ with the CBS-B3LYP method in the gas phase; Table S7: ^1H NMR isotropic magnetic shielding (σ) and chemical shifts (δ) in ppm for the complexes (**VL1–VL4**)·(**H_2O**)$_{8+SMD}$ with the CBS-B3LYP method including H_2O solvation with the Solvation Model based on Density (SMD); Table S8: ^{13}C NMR isotropic magnetic shielding (σ) and chemical shifts (δ) in ppm for complexes (**VL1–VL4**)·(**H_2O**)$_8$ using the CBS-B3LYP method in the gas phase; Table S9: ^{51}V NMR isotropic magnetic shielding (σ) and chemical shifts (δ) in ppm for the complexes (**VL1–VL4**)·(**H_2O**)$_8$ using the CBS-B3LYP method in the gas phase; Table S10: ^{51}V NMR chemical shifts (δ) in ppm for the complexes (**VL1–VL4**)·(**H_2O**)$_8$ using the CBS-B3LYP method in the gas phase.

Acknowledgements L. Noriega thanks CONACYT (Mexico) for financial support (Ph.D. fellowship CVU: 697889). The authors thankfully acknowledge the computer resources, technical expertise and support provided by the Laboratorio Nacional de Supercómputo del Sureste de México, the CONACYT network of national laboratories, the computer resources of the Laboratorio de Supercómputo y Visualización en Paralelo at the Universidad Autónoma Metropolitana-Iztapalapa, and the Project 100256733-VIEP 2019 (VIEP-BUAP, Mexico) as well as the PRODEP Academic Group BUAP-CA-263 (SEP, Mexico).

References

1. Pessoa JC, Etcheverry S, Gambino D (2015) Vanadium compounds in medicine. Coord Chem Rev 301–302:24–48
2. Urquiola C, Vieites M, Aguirre G, Marín A, Solano B, Arrambide G, Nobñía P, Lavaggi ML, Torre MH, González M, Monge A, Gambino D, Cerecetto H (2006) Improving anti-trypanosomal activity of 3-aminoquinoxaline-2-carbonitrile *N*1,*N*4-dioxide derivatives by complexation with vanadium. Bioor Med Chem 14–16:5503–5509
3. Patel MN, Patel SH, Chhasatia MR, Parmar PA (2008) Five-coordinated oxovanadium(IV) complexes derived from amino acids and ciprofloxacin: synthesis, spectral, antimicrobial, and DNA interaction approach. Bioorg Med Chem Lett 18:6494–6500
4. Rivadeneira J, Barrio DA, Arrambide G, Gambino D, Bruzzone L, Echeverry SB (2009) Biological effects of a complex of vanadium(V) with salicyladehyde semicarbazone in osteoblasts in culture: mehcanism of action. J Inorg Biochem 103:633–642
5. Bishayee A, Waghray A, Patel MA, Chatterjee M (2010) Vanadium in the detection, prevention and treatment of cancer: the in vivo evidence. Cancer Lett 294:1–12
6. Gambino D (2011) Potentiality of vanadium compounds as antiparasitic agents. Coord Chem Rev 255:2193–2203
7. Crans DC, Tarlton ML, McLauchlan CC (2014) Trigonal bipyramidal or square pyramidal coordination geometry? Investigating the most potent geometry for vanadium phosphatase inhibitors. Eur J Inorg Chem 27:4450–4468
8. Banerjee S, Dixit A, Karande AA, Chakravarty AR (2016) Endoplasmic reticulum targeting tumour selective photocytotoxic oxovanadium(IV) complexes having vitamin-B6 and acridinyl moieties. Dalton Trans 45:783
9. Bijelic A, Aureliano M, Rompel A (2018) The antibacterial activity of polyoxometalates: structures, antibiotic effects and future perspectives. Chem Commun 54:1153
10. Zhou QC, Wang TR, Li H, Chen L, Xin JJ, Guo S, Sheng GH, You ZL (2019) Synthesis, crystal structures and insulin-like activity of three new oxidovanadium(V) complexes with aroylhydrazone ligand. J Inorg Biochem 196:110680
11. El-Deen IM, Shoair AF, El-Bindary MA (2019) Synthesis, characterization and biological properties of oxovanadium(IV) complexes. J Mol Struct 1180:420–437
12. Ebrahimipour SY, Sheikhshoaie I, Kautz AC, Ameri M, Pasban-Aliabadi H, Rudbari HA, Bruno G, Janiak C (2015) Mono-and dioxido-vanadium(V) complexes of tridentate ONO Schiff base ligand: synthesis, spectral characterization, X-ray structure, and anticancer activity. Polyhedron 93:99–105
13. Ronconi L, Sadler PJ (2008) Applications of heteronuclear NMR spectroscopy in biological and medicinal inorganic chemistry. Coord Chem Rev 252:2239–2277
14. Rehder D (2008) Vanadium NMR of organovanadium complexes. Coord Chem Rev 252:2209–2222
15. Dapprich S, Komáromi I, Byun KS, Morokuma K, Frisch MJ (1999) A new ONIOM implementation in Gaussian 98. 1. The calculation of energies, gradients and vibrational frequencies and electric field derivatives. J Mol Struct (Theochem) 462:1–21. https://doi.org/10.1016/s0166-1280(98)00475-8
16. Hohenberg P, Kohn W (1964) Inhomogeneous electron gas. Phys Rev 136:B864–B871
17. Roothaan CCJ (1951) New developments in molecular orbital theory. Rev Mod Phys 23:69

18. Peterson KA, Woon DE, Dunning TH Jr (1994) Benchmark calculations with correlated molecular wave functions. IV. The classical barrier height of the H + H2 → H2 + H reaction. J Chem Phys 100:7410–7415
19. Dunning TH Jr (1989) Gaussian basis sets for use in correlated molecular calculations. I. The atoms boron through neon and hydrogen. J Chem Phys 90:1007–1023
20. Schaefer A, Horn H, Ahlrichs R (1992) Fully optimized Gaussian basis sets for atoms Li to Kr. J Chem Phys 97:2571–2577
21. Miliordos E, Aprà E, Xantheas SS (2014) Benchmark theoretical study of the π–π binding energy in the benzene dimer. J Phys Chem A 118:7568–7578
22. He N, Li ZH (2016) Palladium-atom catalyzed formic acid decomposition and the switch of reaction mechanism with temperature. Phys Chem Chem Phys 8:10005–10017
23. Jorgensen KR, Cadena M (2018) Theoretical study of bromide halocarbons: accurate enthalpies of formation. Comp Theor Chem 1141:66–73
24. Kupka T, Ruscic B, Botto RE (2002) Toward hartree-fock- and density functional complete basis-set-predicted NMR parameters. J Phys Chem A 106:10396–10407
25. Kupka T (2008) From correlation-consistent to polarization-consistent basis sets estimation of NMR spin–spin coupling constant in the B3LYP Kohn–Sham basis set limit. Chem Phys Lett 461:33–37
26. Kupka T, Lim C (2007) Polarization-consistent versus correlation-consistent basis sets in predicting molecular and spectroscopic properties. J Phys Chem A 111:1927–1932
27. Melendez FJ, Castro ME, Perez-Aguilar JM, Caballero NA, Noriega L, González-Vergara E (2018) Computational study of aqueous solvation of vanadium(V) complexes. In: Conference proceedings of international supercomputing conference in México (ISUM 2018), vol CCIS 948. Springer, Berlin
28. Marenich AV, Cramer CJ, Truhlar DG (2009) Universal solvation model based on solute electron density and a continuum model of the solvent defined by the bulk dielectric constant and atomic surface tensions. J Phys Chem B 113:6378–6396
29. Zhao Y, Truhlar DG (2008) The M06 suite of density functionals for main group thermochemistry, thermochemical kinetics, noncovalent interactions, excited states, and transition elements: two new functionals and systematic testing of four M06-class functionals and 12 other functionals. Theor Chem Acc 120:215–241
30. Jeffrey HP, Wadt WR (1985) Ab initio effective core potentials for molecular calculations. Potentials for main group elements Na to Bi. J Chem Phys 82:299–310
31. Zhang RB, Ai XC, Zhang XK, Zhang QY (2004) Solvent effects on the excited state properties of 2-aminopurine—a theoretical study by the ONIOM and supramolecular method. J Mol Struct (Theochem) 680:21–27
32. Da Silva EF, Svendsen HF, Merz KM (2009) Explicitly representing the solvation shell in continuum solvent calculations. J Phys Chem A 113(22):6404–6409
33. Pedone A, Bloino J, Monti S, Prampolini G, Barone V (2010) Absorption and emission UV–Vis spectra of the TRITC fluorophore molecule in solution: a quantum mechanical study. Phys Chem Chem Phys 12:1000–1006
34. Becke AD (1993) Density-functional thermochemistry. III. The role of exact exchange. J Chem Phys 98:5648–5652
35. Cheeseman JR, Trucks GW, Keith TA, Frisch MJ (1996) A comparison of models for calculating nuclear magnetic resonance shielding tensors. J Chem Phys 104:5497–5509
36. Frisch MJ, Trucks GW, Schlegel HB, Scuseria GE, Robb MA, Cheeseman JR, Scalmani G, Barone V, Mennucci B, Petersson GA, Nakatsuji H, Caricato M, Li X, Hratchian HP, Izmaylov AF, Bloino J, Zheng G, Sonnenberg JL, Hada M, Ehara M, Toyota K, Fukuda R, Hasegawa J, Ishida M, Nakajima T, Honda Y, Kitao O, Nakai H, Vreven T, Montgomery JA, Peralta JE Jr, Ogliaro F, Bearpark M, Heyd JJ, Brothers E, Kudin KN, Staroverov VN, Kobayashi R, Normand J, Raghavachari K, Rendell A, Burant JC, Iyengar SS, Tomasi J, Cossi M, Rega N, Millam JM, Klene M, Knox JE, Cross JB, Bakken V, Adamo C, Jaramillo J, Gomperts R, Stratmann RE, Yazyev O, Austin AJ, Cammi R, Pomelli C, Ochterski JW, Martin RL, Morokuma K, Zakrzewski VG, Voth GA, Salvador P, Dannenberg JJ, Dapprich S, Daniels AD, Farkas Ö, Foresman JB, Ortiz JV, Cioslowski J, Fox DJ (2009) Gaussian, Inc., Wallingford, CT
37. X-ray crystallographic data from http://www.ccdc.cam.ac.uk/ (last accessed Jan 17, 2017) or from the Cambridge Crystallographic Data Centre, 12, Union Road, Cambridge CB2 1EZ, UK
38. Sheppard BJH, Shaver MP, Pearson JK (2015) Assessment and application of density functional theory for the prediction of structure and reactivity of vanadium complexes. J Phys Chem A 119:8537–8546
39. Humphrey W, Dalke A, Schulten K (1996) VMD—visual molecular dynamics. J Mol Graph 14:33–38
40. Melendez FJ, Degollado A, Castro ME, Caballero NA, Guevara-García JA, Scior T (2014) Theoretical study of the structure, IR and NMR of the bis-peroxo-oxovanadate species containing-histidine peptides. Inorg Chim Acta 420:149–158
41. Maurya MR, Kumar A, Bhat AR, Azam A, Bader C, Rehder D (2006) Dioxo- and oxovanadium(V) complexes of thiohydrazone ONS donor ligands: synthesis, characterization, reactivity, and atiamoebic activity. Inorg Chem 45:1260–1269
42. Kwiatkowski E, Romanowski G, Nowicki W, Kwiatkowski M, Suwinska K (2003) Dioxovanadium(V) Schiff base complexes of *N*-methyl-1,2-diaminoethane and 2-methyl-1,2-diaminopropane with aromatic *o*-hydroxyaldehydes and *o*-hydroxyketones: synthesis, characterization, catalytic properties and structure. Polyhedron 22:1009–1018
43. Lippold I, Becher J, Klemm D, Plass W (2009) Chiral oxovanadium(V) complexes with a 6-amino-6-deoxyglucopyranoside-based Schiff-base ligand: catalytic asymmetric sulfoxidation and structural characterization. J Mol Catal A Chem 299:12–17
44. Maurya MR, Kumar A, Ebel M, Rehder D (2006) Synthesis, characterization, reactivity, and catalytic potential of model Vanadium(IV, V) complexes with benzimidazole-derived ONN donor ligands. Inorg Chem 45:5924–5937
45. Romanowski G, Wera M (2010) Mononuclear and dinuclear chiral vanadium(V) complexes with tridentate Schiff bases derived from *R*(-)-1,2-diaminopropane: synthesis, structure, characterization and catalytic properties. Polyhedron 29:2747–2754
46. Guevara G, Behrens NB, Contreras R, Mendoza D (1998) In: Tracey S, Crans DC (eds) Vanadium compounds. chemistry, biochemistry, and therapeutic applications, vol 711. American Chemical Society, Washington, DC, p 126
47. Cramer CJ, Truhlar DG (1999) Implicit solvation models: equilibria, structure, spectra, and dynamics. Chem Rev 99(8):2161–2200
48. Guthrie JP (2009) A blind challenge for computational solvation free energies: introduction and overview. J Phys Chem B 113(14):4501–4507
49. Caravan P, Gelmini L, Glober N, Herring FG, Li H, McNeill JH, Rettig SJ, Setyawati IA, Shuter E, Sun Y, Tracey AS, Yuen VG, Orvig C (1995) Reaction chemistry of BMOV, bis(maltolato) oxovanadium(IV)—a potent insulin mimetic agent. J Am Chem Soc 117:12759–12770

Affiliations

Lisset Noriega[1] · María Eugenia Castro[2] · Jose Manuel Perez-Aguilar[1] · Norma A. Caballero[3] · Thomas Scior[4] · Ramsés E. Ramírez[5] · Enrique González-Vergara[2] · Francisco Javier Meléndez[1]

[1] Lab. de Química Teórica, Centro de Investigación, Depto. de Fisicoquímica, Facultad de Ciencias Químicas, Benemérita Universidad Autónoma de Puebla, Edif. FCQ10, 22 Sur y San Claudio, Ciudad Universitaria, Col. San Manuel, 72570 Puebla, Mexico

[2] Centro de Química, Instituto de Ciencias, Benemérita Universidad Autónoma de Puebla, Complejo de Ciencias, ICUAP, Edif. IC8, 22 Sur y San Claudio, Ciudad Universitaria, 72570 Puebla, Puebla, Mexico

[3] Facultad de Ciencias Biológicas, Benemérita Universidad Autónoma de Puebla, Edif. BIO1, 22 Sur y San Claudio, Ciudad Universitaria, Col. San Manuel, 72570 Puebla, Mexico

[4] Depto. de Farmacia, Facultad de Ciencias Químicas, Benemérita Universidad Autónoma de Puebla, 14 Sur y San Claudio, Ciudad Universitaria, Col. San Manuel, 72570 Puebla, Mexico

[5] Depto. de Fisicomatemáticas, Facultad de Ciencias Químicas, Benemérita Universidad Autónoma de Puebla, Edif. FCQ10, 22 Sur y San Claudio, Ciudad Universitaria, Col. San Manuel, 72570 Puebla, Mexico